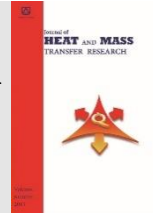




Semnan University



Research Article

Monte Carlo Optimization of a Solar Combisystem Using Photovoltaic-Thermal Systems in Hot and Dry Climatic Condition

Maryam Karami ^{*,a}, Kiavash Akbari ^b, Mohammad Jalalizadeh ^b

^aDepartment of Mechanical Engineering, Faculty of Engineering, Kharazmi University, Tehran, Iran

^bDepartment of Architectural Technology, Faculty of Architecture and Urbanism, University of Art, Tehran, Iran

PAPER INFO

Paper history:

Received: 2022-09-19

Revised: 2023-03-10

Accepted: 2023-03-14

Keywords:

Solar combisystem;
Photovoltaic-thermal system;
Dynamic simulation;
Monte Carlo optimization;
TRNSYS.

ABSTRACT

In this study, the performance of a solar combisystem using glazed thermal photovoltaic-thermal systems is investigated and optimized to provide the thermal and electrical demands of a five-story building in Hot/Dry climatic conditions (Tehran, Iran). Dynamic simulation of the system performance is carried out using TRNSYS software. Since there is no type for a glazed thermal photovoltaic-thermal system in TRNSYS, it is modeled in MATLAB software and then the modeling results are coupled with the TRNSYS model. The system optimization using a stochastic economic analysis based on the Monte Carlo method showed the solar combisystem with a photovoltaic-thermal system area of 31.93 m² and a thermal storage tank of 400 l provides the building energy demands optimally. For the optimum system, the probability that the payback time is less than 5 years, the internal rate of return is more than 20% and the life cycle savings is more than the initial cost is 74.2%, 11.5%, and 97%, respectively. The thermoelectric analysis of the optimum solar combisystem indicates that, in August, the maximum electrical, thermal, and total solar fractions of the system are obtained, which are 11%, 87%, and 39%, respectively.

DOI: [10.22075/jhmtr.2023.28432.1394](https://doi.org/10.22075/jhmtr.2023.28432.1394)

© 2022 Published by Semnan University Press. All rights reserved.

1. Introduction

Using renewable energy as an alternative to fossil fuels due to the environmental and economic advantages is one of the ways to reduce energy consumption. Among the types of renewable energy, solar energy is the most widely used source of renewable energy in the world [1,2]. With 300 sunny days a year, Iran is one of the best countries in the world in terms of solar energy potential, and considering the geographical location of Iran and rural distribution in the country, the use of solar energy is one of the most important factors to be considered [3].

In recent years, the application of solar thermal energy in the residential sector has significantly developed. This is because this sector needs a medium

temperature level that can be provided by the solar system [4,5]. Formerly, solar thermal systems were used only to supply domestic hot water (DHW) load; however, with the development of low-temperature heating systems, such as underfloor heating, the use of solar combisystem (SCS) to provide part of the space heating (SH) load of the buildings was also developed. For example, Leckner and Zmeureanu [6] presented a net zero energy house using an SCS. Results showed that the energy payback ratio of the SCS is 3.5–3.8 compared with the conventional heating system and financial payback is never attained because of the high cost of the SCS and the low cost of electricity in Montreal, Canada. Asaee et al. [7] investigated the potential of SCSs in Canadian houses and found that by

*Corresponding Author: Maryam Karami.

Email: karami@khu.ac.ir

increasing collector area, SCS solar fraction is improved. Performance Comparison of an SCS and solar water heater (SWH), done by Sustar et al. [8], shows that the energy savings by an SCS compared to an SWH is as high as 8% for a 6 m² system and 27% for a 9 m² system where relatively high solar radiation is available during the cold season. To provide the heating needs of Tunisian households, Mehdaoui et al. [9] have compared two solar heating technologies: a solar heating system with an integrated active layer on the floor and in the wall. The optimal size of the heating system that provides the maximum solar fraction includes a solar collector with an area of 6 m², a mass flow of 120 kg/h, a 450 l storage tank, and a mass flow within the layer of 300 kg/h. A comparison of the long-term performance of the solar heating systems showed that the use of the floor results in a high solar fraction of about 78%. In another study, Hazami et al. [10] simulated the operation of an SCS to generate electricity and heat using TRNSYS software for Tunisian weather conditions. The results showed that the SCS provides 20% to 40% of the energy required for space heating and 40% to 70% of the energy needed for the DHW. Also, using the SCS, electricity generation between 32 and 225 MJ/m² is obtained. Katsaprakakis and Zidianakis [11] investigated an SCS for heating a school on the Greek island of Crete with biomass fuel. In this study, the building has two desirable features: geographical location with appropriate sunlight and according to school hours (morning shift), all the required thermal energy can be provided by the combisystem, and energy during holidays is stored in a heat storage tank. The two desirable properties mentioned above lead to solar energy supplying more than 50% of the required energy. The effect of weather conditions on the performance of the SCS using the underfloor heating system is investigated by Karami and Javanmardi [12]. They reported that the annual solar fraction in Hot/Dry, Cold/Dry, Moderate/Humid, Hot/semi Humid, and Hot/Humid climates are 74%, 61%, 47.8%, 87.9%, and 92%, respectively. Using a TRNSYS-MATLAB co-simulator, Karami and Nasiri Gahrzaz [13] simulated the thermal performance of an SCS in a Hot/Dry climate using two solar collectors including the flat plate solar collector (FPSC) and a nanofluid-based direct absorption solar collector (DASC) [14, 15]. The results indicate that using FPSC, the annual energy consumption for providing DHW and SH loads using the proposed SCS reduces 94.3% and 17%, respectively. In the case of using a DASC, the solar fraction for DHW and SH in comparison with nanofluid-based DASC increases by 3.7% and 1.7%, respectively. They also considered the thermoelectric and economic performance of the SCS using photovoltaic-thermal (PVT) systems as the energy source [13]. They found that the annual solar fraction of DHW and SH increased 11.3% and 15.6%,

respectively, because of using the electrical energy generated by the system. Based on the results of the economic analysis, the fuel saving cost of 29479 \$ is obtained during the life cycle of the SCS, and the payback period is 3.75 years [16]. Kannan et al. [17] designed and evaluated an off-grid solar combisystem using phase change materials. Their results show that the average energy saving ratio for space heating is about 93%, respectively. Also, the air temperature in the phase change material (PCM) integrated space unit is 4 to 6 °C cooler than that without PCM integrated space unit.

There are several studies on the optimization of SCSs. Bornatico et al. [18] proposed a method for finding the optimal size of the main components of an SCS using the particle swarm optimization (PSO) algorithm and compared the results with the genetic algorithm-based optimization framework. They concluded that the PSO method is a slightly better choice. The optimal size of the main components is the solar collector with an area of 14.5 m², a tank volume of 498.98 l, and an auxiliary power unit of 8.5 kW. The optimized system has a solar fraction of 21.8%, a total energy consumption equivalent to 15806 kWh and an installation cost of 8,983 €. Hin et al. [19] optimized a residential SCS for a house in Montreal, using a hybrid PSO and Hook-Jeeves generalized pattern search algorithm (PSO/HJ) to minimize the life cycle cost (LCC), life cycle energy (LCE) consumption, and life cycle destroyed exergy (LCX) of the system. The optimized system reduces the LCC by 19% and the LCE consumption by 34% compared to the base SCS. The exergy payback time of all system configurations is between 4.2 and 6.3 years. Rey and Zmeureanu [20] used two objective functions, LCC and LCE, to optimize the SCS in Montreal, Canada. Two different approaches including a weight sum method using a PSO/HJ and multi-objective PSO are presented and compared to solve such problems. Finally, the multi-purpose PSO was selected because it was up to six times faster than the PSO/HJ. By different design options of the multi-objective PSO/HJ, LCC and LCE were reduced to 88.6% and 63.9%, respectively, in comparison with the base case SCS. In the next study, they used micro-time variant multi-objective PSO (micro-TVMOPSO) to optimize the performance of an SCS and reported that the number of solar collectors has the most effect on both LCC and LCE [21]. They also selected the SCSs with different configuration capabilities and then investigated the LCC, LCE consumption, and LCX were investigated using the method of micro-TVMOPSO. To minimize LCC, only one FPSC with one storage tank is required, while seven evacuated tube solar collectors (ETSC) and two storage tanks are used for minimum LCE consumption. However, such an improvement requires an additional cost that is not worth much for such economic conditions [22]. Using taguchi method, Li and Kao [23] optimized solar thermal and heat

pump combisystems under five distinct climatic conditions including Tropical monsoon (Tainan), Continental (Madrid), Humid subtropical (Osaka), Humid subtropical (Hong Kong), and Mediterranean (Lisbon). They reported that Tainan and Lisbon have the longest and shortest payback period because of lower and higher electricity price, respectively. Thapa et al. [24] designed, modeled, and optimized an SCS for single-family houses in Nepal. Optimization variables include collector area, DHW, and SH storage tank size. The dynamic simulation using TRNSYS software and PSO method is used for optimization. This system is simulated in two regions including Terai and Hilli with different climates in Nepal. In Tray, has a system with an area of 6 m² of solar collector, DHW, and storage tank with a volume of about 130 l, and in Hilli, a collector with an area of 14 m² and tanks with a volume between 150 l and 170 l are optimum. The LCC of the SCS is reduced by 66% in Terai and 77% in Hilli. A summary of the SCS optimization studies are listed in Table 1.

As the review shows, earlier studies use deterministic economic analysis to optimize the SCSs and ignore the uncertainties in model inputs, which undoubtedly result in uncertainties in model outputs. Therefore, in this study, the SCS is optimized using a stochastic economic analysis based on the Monte Carlo method, in which the uncertainty is considered by designating inputs as probability distributions. Furthermore, the thermoelectric performance of the optimum SCS in Hot and Dry climatic conditions (Tehran, Iran) is investigated using dynamic simulation by TRNSYS-MATLAB cosimulator.

2. Case study building and SCS description

In this study, a five-story building located in Hot/Dry climatic conditions (Tehran, Iran) is selected as the case study building. Figure 1 shows the hourly variation of the ambient temperature and solar radiation of Tehran. Each floor of the building consists of two residential units with a 143 m² area and 4 occupants. The characteristics of the building are shown in Table 2. The daily DHW consumption for each person is considered 50 l.

To determine the electrical, DHW, and SH loads of the building, it is first necessary to simulate the building in Design-Builder software. The annual DHW, SH, and electrical loads of the building are obtained 32.57 MWh, 89.57 MWh, and 60.18 kW, respectively. It should be noted that the building has no central HVAC equipment and instead uses an evaporative cooler for cooling and a packaged gas fired heater for heating. Also, the electrical load and operation schedule of electrical equipment are introduced to the software based on Iranian National Building Code-No.19.

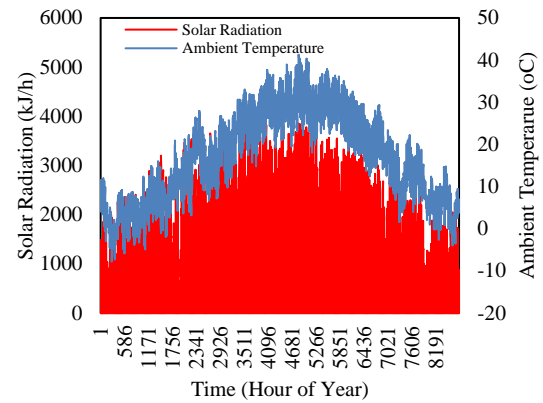


Figure 1. Hourly variation of ambient temperature and solar radiation in Tehran

In this study, the proposed system to supply DHW, SH, and electricity for a building in Tehran (35.7219° N, 51.3347° E) is a PVT-based SCS. Figure 2 shows the schematic of the proposed system. In this system, the heated working fluid in the PVT systems divides between the DHW and SH tanks, exchanges heat with water in the tanks, and then, the cooled working fluid returns from the tanks and enters the PVT system to continue this cycle. The hot water in the SH tank enters the boiler to reach the appropriate temperature for providing the SH load. If the water in the DHW tank is not at the desired temperature, the auxiliary heater inside the tank turns on and heats the water to the set-point temperature.

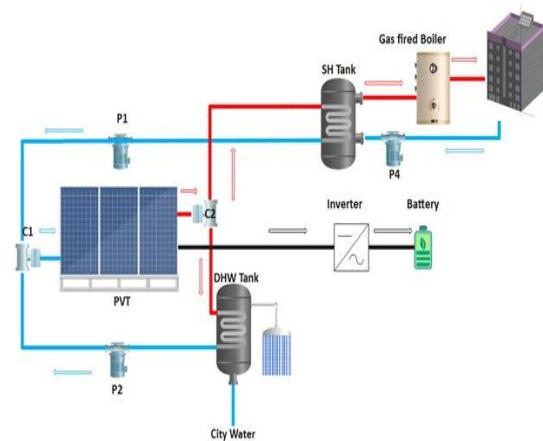


Figure 2. Schematic of the proposed PVT-based SCS

3. Methodology

The flowchart in Figure 3 indicates the process of the simulation and optimization study of the SCS. As shown, the simulation process is divided into two parts: thermoelectric and economic simulations. First, using basic information and TRNSYS software, the thermoelectric simulation is carried out, and then the results are entered the Crystal ball software so that the economic calculations for the considered SCS is carried out using Monte Carlo method.

Table 1. Summary of SCS optimization studies

Ref.	Optimization method	Optimization objectives	Climatic conditions	Findings
Bornatico et al. [18]	PSO algorithm and GA	<ul style="list-style-type: none"> • Collector area • Tank volume • Auxiliary power unit 	Zurich, Switzerland	<ul style="list-style-type: none"> • Collector size is the most important parameter. • Solar fraction of 21.8% for a mid-sized single-family house (150 m²) using collector area of 14.5 m², tank volume of 498.98 l, and an auxiliary power unit of 8.5 kW.
Hin et al. [19]	Hybrid PSO/HJ	<ul style="list-style-type: none"> • LCC • LCE consumption • LCX 	Montreal, Quebec, Canada	<ul style="list-style-type: none"> • Reduction of the LCC by 19% and the LCE consumption by 34%. • The exergy payback time is between 4.2 and 6.3 years.
Rey and Zmeureanu [20]	<ul style="list-style-type: none"> • Hybrid PSO/HJ • MOPSO • Hybrid MOPSO/HJ 	<ul style="list-style-type: none"> • LCC • LCE use 	Montreal, Quebec, Canada	<ul style="list-style-type: none"> • PSO/HJ method is time-consuming, while MOPSO/HJ was more than six times faster. • Collector size and mass flow rate has high and small influence on thermal energy savings, respectively.
Rey and Zmeureanu [21]	<ul style="list-style-type: none"> • Micro-MOPSO • Micro-TVMOPSO 	<ul style="list-style-type: none"> • LCC • LCE use 	Montreal, Quebec, Canada	<ul style="list-style-type: none"> • Micro-TVMOPSO algorithm performed better than other optimization algorithms. • Optimum tilt angle for solar collector is 45° for Montreal.
Rey and Zmeureanu [22]	Micro-TVMOPSO	<ul style="list-style-type: none"> • LCC • LCE consumption • LCX 	Montreal, Quebec, Canada	<ul style="list-style-type: none"> • To minimize LCC, only one FPSC with one storage tank is required, while seven evacuated tube solar collectors (ETSC) and two storage tanks are used for minimum LCE consumption.
Li and Kao [23]	Taguchi	<ul style="list-style-type: none"> • COP of heat pump • Solar fraction of SCS 	<ul style="list-style-type: none"> • Tropical monsoon (Tainan) • Continental (Madrid) • Humid subtropical (Osaka) • Humid subtropical (Hong Kong) • Mediterranean (Lisbon) 	<ul style="list-style-type: none"> • For single tank SCS, the flow rate of heat pump has the high impact, while for dual tank SCS, the flow rate of the collector is most influential. • Tainan and Lisbon have the longest and shortest payback period because of lower and higher electricity price, respectively
Thapa et al. [24]	Hybrid PSO/HJ	<ul style="list-style-type: none"> • Collector area • DHW storage tank size • SH storage tank size 	<ul style="list-style-type: none"> • Terai, Nepal • Hilli, Nepal 	<ul style="list-style-type: none"> • The LCC of the SCS is reduced by 66% in Terai and 77% in Hilli, respectively. • The building envelope insulation plays a key role in the wide use of SCS in Nepal.

Table 2. Characteristics of the case study building

Characteristics	Value
Orientionation	South
External wall U value (W/m ² .K)	1.28
Internal wall U value (W/m ² .L)	1.85
Floor U value (W/m ² .K)	2.23
Roof U value (W/m ² .K)	2.23
Window glazing U value (W/m ² .K)	3.09
The ratio of Windows-to-Wall ratio (%)	20
Infiltration rate (Ach)	0.7

3.1. Thermoelectric analysis

Figure 4 indicates the TRNSYS model of the PVT-based SCS. In Table 3, the TRNSYS types used in the simulation and their characteristics are listed. It should be noted that Type 109 was used to read weather data from the Typical Meteorological Year (TMY) files and

calculates the solar radiation in different directions. System controllers (Type 2b) were used to control the flow rate of the collectors and the storage tanks. For example, if the difference between the outlet and inlet temperature of the collector is less than 5°C, the collector loop pump will be turned off. Also, if the difference exceeds 10°C, the pump will turn on. Type 14b is used to simulate the daily DHW demand, of which profile is obtained in Ref. [12]. As mentioned, the cooling and heating loads of the case study building are obtained using Design Builder modeling and the results are coupled with TRNSYS using Type 9e, which calls the calculated thermal and electrical loads by linking to an external excel file.

Since there is no type for the glazed PVT systems, a model is developed in MATLAB software and then, connected to the TRNSYS model using Type 155. The details of the modeling of the glazed PVT systems can be obtained in Ref. [25].

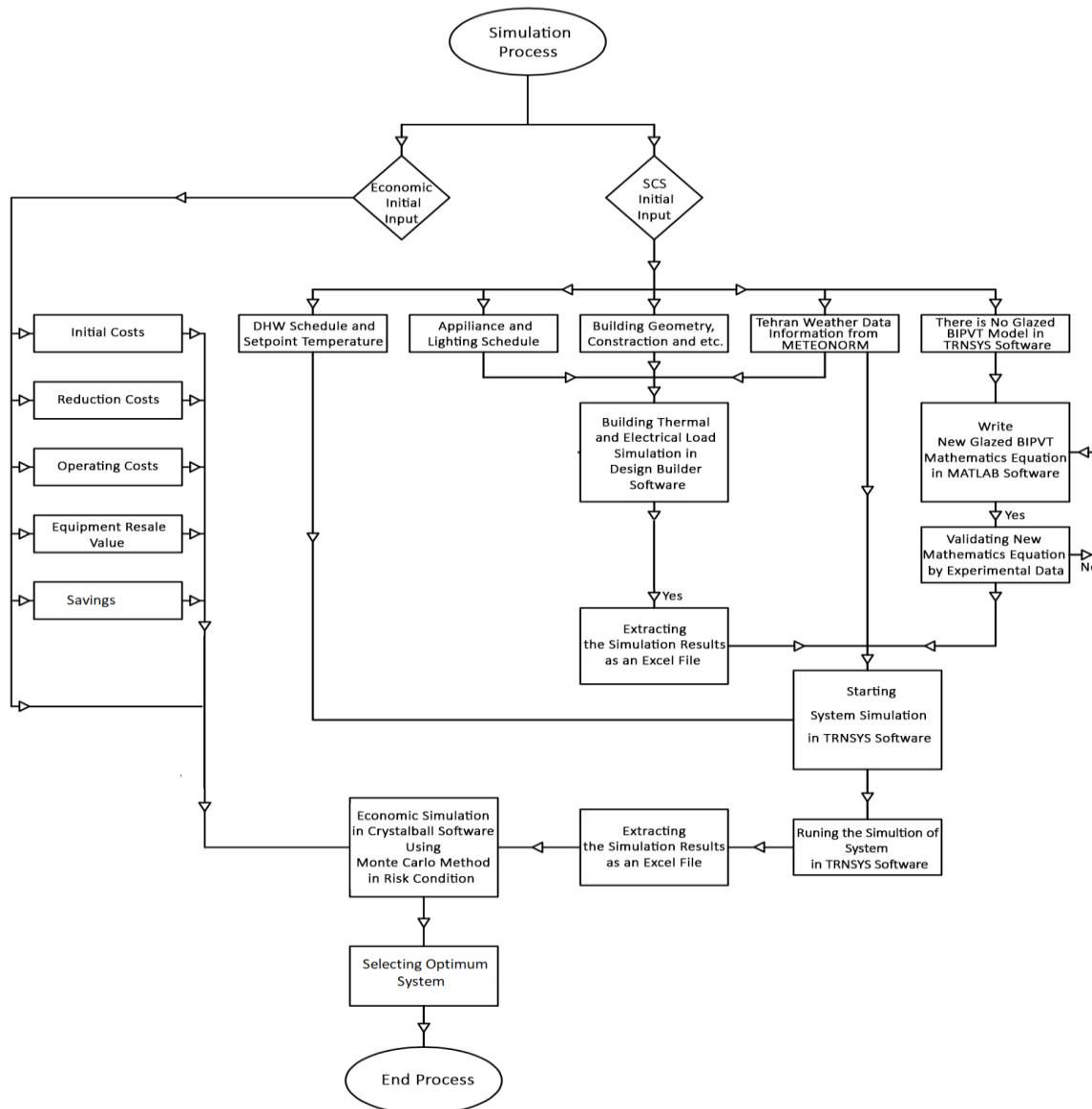


Figure 3. Flow chart diagram of the SCS simulation

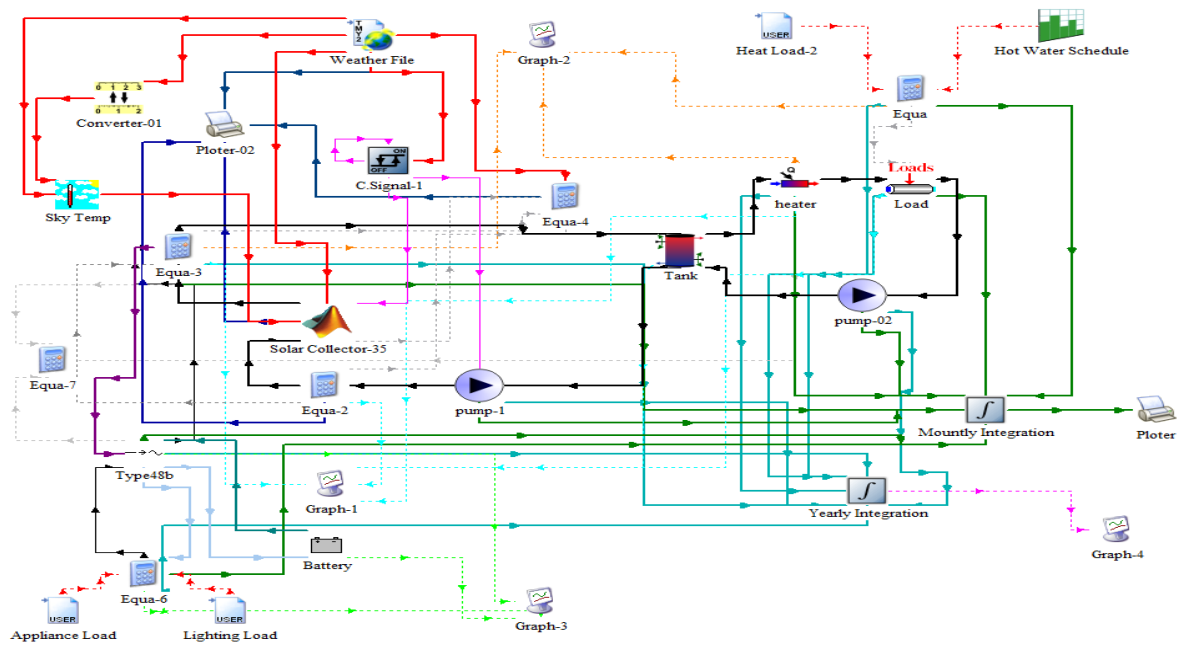


Figure 4. TRNSYS model of the SCS

Table 3. TRNSYS types for modeling the SCS components

Component	Features	TRNSYS type
Case study building	See Section 2	56
Weather information	Tehran, Iran (35.7219° N, 51.3347° E)	109
Sky temperature	---	69
Psychrometric properties	Such as dew point, relative humidity, etc.	33
Glazed PVT systems	BIPVT collector mass flow rate: 50 kg/h Fluid Type: Water	155
Electrical inverter	Inverter output power capacity: 42 kW Regulator efficiency: 0.8 Inverter efficiency: 0.96	48a
Battery	Cell efficiency capacity: 200 Wh Number of cells in parallel: 24 Number of cells in series: 12 Charging efficiency: 0.9	47a
Circulation Pumps	Power coefficient: 0.5 Maximum power: 1 kw Maximum flowrate: 1590 kg/h	3b
Storage tanks	Six thermal nodes level with the same constant flow rate are defined for the thermal storage tank Thermal storage tank loss coefficient: 0.83 W/m ² . K	4
Auxiliary heater	Maximum hear rate: 100 kW Set point temperature: 80°C Efficiency: 0.9	6
DHW	Set point temperature: 60°C	14b
Controllers	Controller type: Feedback controller	2b
Flow diverter and mixing valve	---	11 and 11 h
Cooling and heating load	Calling Excel	9e
Plotter, Printer, and Integrator	---	65d, 25a, and 24

3.2. Economic analysis using Monte Carlo approach

In this study, the Monte Carlo method is used for the economic analysis of the proposed SCS. In general, the Monte Carlo method refers to a computational mathematical technique that provides approximate answers to quantitative problems through statistical sampling. It is mostly used to describe propagating uncertainties in model input and to analyze uncertainties in model output. The Monte Carlo method, then, is a kind of simulation that explicitly and quantitatively shows uncertainty by designating inputs as probability distributions. If the inputs describing a system are uncertain, then the prediction of the performance is essentially uncertain. This means that the result of any analysis based on inputs with probability distribution is itself a probability distribution [26,27].

To show the effect of the price inflation rate during the life of the proposed system, normal distribution was used in the simulation in the stochastic approach of the Monte Carlo method. The electricity and natural gas prices can also change over the life of the system. For this reason, in the calculations, the normal distribution is also used for the price growth of these energy sources. The inflation rate of the discount rate is considered by a triangle distribution with a maximum value of 0.16, a minimum value of 0.10, and a mean value of 0.13. A triangle distribution is used to distribute variables when the minimum and maximum values are constant and the highest probability is different from the other probabilities. As the discount rate is variable, the maintenance cost is also variable, and since the discount is considered a triangle, a triangle distribution has been used to express the inflation rate of the maintenance cost, the range of which is between 1% and 5% with the highest probability of 3% in the first 5 years of operation. However, from the 5th year of operation, it is between 5% and 15% with the highest probability of 10%.

Table 4 shows the variables and value ranges used for the optimization of the proposed SCS for the case study building. It should be noted that the collector slope is assumed constant and equal to the latitude of Tehran (about 35°).

Table 4. Variables used in this study and their value ranges

Variables	Value ranges
PVT area (m ²)	10.6-138.9
Storage tank volume	300-3000 lit
Collector mass flow rate	512- 13300 kg/h
Auxiliary boiler capacity	25-40 kW
Inverter number	1-5

Table 5 shows the cost of the SCS main components. The initial costs include the initial investment cost (PVT systems and related equipment), the cost reduction of the primary heating systems (the cost of purchasing a boiler with a lower capacity), and installation costs. The operating costs of the system are considered equal to 10% of the initial cost.

Table 5. SCS main component cost

Component	Cost
Total PVT systems (\$)	2280-29640
Inverter (\$)	459-2295
Installation cost (\$)	2128-27785
Total initial cost (\$)	4867-58148
Auxiliary boiler (\$)	2428-4000

3.3. Economic indicators

In this study, four economic indicators including payback time (PBT), net present value (NPV), internal rate of return (IRR), and life cycle savings (LCS) are used which determine the decision criteria for the implementation of the proposed systems. The PBT indicates the time required to return the initial costs, which is calculated using the following relation [28]:

$$\sum_{i=0}^{N_{\min}=DPBP} \frac{F_t}{(1+d)^i} \geq 0 \tag{1}$$

where d is the discount rate. If F₀ is the life cycle cost (LCC) and F_i is the net profit, which is the difference between savings and LCC, then the payback period (N_{min}) will be the lowest. One of the disadvantages of this indicator is the investment conditions after the payback period in such a way that the amount and duration of profitability are not known, so it is necessary to consider other indicators.

The NPV of investment represents the total present value of all expenses and savings of the project. If the NPV is positive, the system is affordable and the project earnings exceed the anticipated costs. If NPV is zero, the earnings are equal to the costs and if it is negative, the system is not affordable [29]. The main disadvantage of this indicator is that it does not provide any information about the initial costs. The NPV can be calculated through Eq. (2):

$$NPV = \sum_{i=0}^N \frac{F_i}{(1+d)^i} \tag{2}$$

The IRR is the interest rate that results in the present value of the expenses equal to the present value of the savings. In fact, the IRR is the interest rate at which the NPV is zero:

$$NPV = \sum_{i=0}^N \frac{F_i}{(1+IRR)^i} = 0 \tag{3}$$

The LCS is the difference between the LCC of a conventional fuel-only system and the LCC of the solar plus auxiliary system [30], which by discounting is calculated as follows:

$$LCS = \sum_{i=0}^N \frac{F_i}{(1+d)^i} \quad (4)$$

4. Results and discussion

4.1. Optimization analysis using Monte Carlo algorithm

The incomes of the lifetime include the electricity generated and the natural gas saved which is given in Figure 5. The equipment resale value, which is equal to 25% of the initial cost of the system, is also an income. It is a recovery value, which is returned during the life of the system or at the end of it when the components are sold as scrap metal for recycling [30]. It should be mentioned that the variable price of gas and electricity are included in the Monte Carlo method.

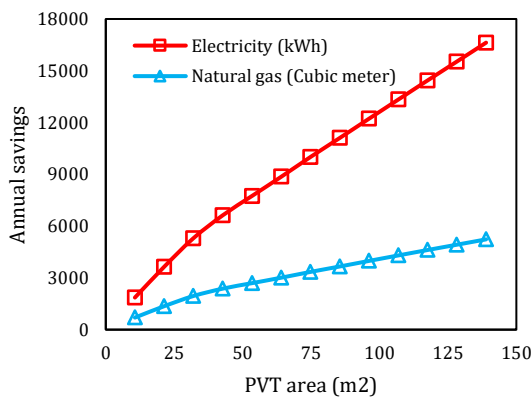


Figure 5. Annual electricity and natural gas savings for different SCSs

By determining the distribution of the variables using the Monte Carlo method, the LCS, PBT, and IRR indicators are calculated. To analyze the LCS in risky conditions, a suitable criterion is needed. The best criterion for showing the optimality of this indicator is the probability that it is higher than the initial costs of the system (Table 5).

Figure 6 shows the PBT, IRR, and LCS indicators, taking into account the probability of the PBT, the IRR, and the LCS are less than 5 years, less than 20%, and more than system’s initial cost, respectively. As can be seen, the optimum indicators are obtained using the SCS with a PVT area of about 31.9 m². Table 6 shows the various economic indicators for the optimum SCS.

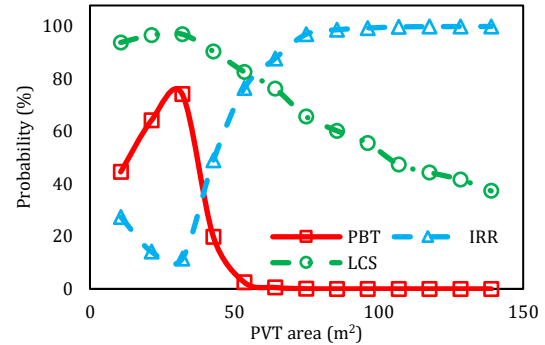


Figure 6. Probability of the PBT (less than 5 years), IRR (less than 20%) and LCS (more than initial cost)

Table 6. Features of the optimum SCS

Feature	Value
PVT area	31.9 m ²
Collector mass flow rate	1536 kg/h
Thermal Storage Tank Volum	400 l
Inverter No.	1
Auxiliary Boiler Capacity	35 kW
Probability of PBT less than 5 years	74.2%
Probability of IRR less than 20%	11.5%
Probability of LCS more than initial cost	97%

4.2. Optimization analysis using Monte Carlo algorithm

Figure 7 shows the monthly variation of incident solar radiation and electrical energy generation (EEG), electrical energy consumption (EEC), and electrical energy received from the grid (EER_Grid). It is observed that by increasing the solar radiation, the EEG also increases; so that more EEG is obtained in warm months and as a result, EER_Grid is reduced. As can be seen, the highest incident radiation and EEG are 207.83 kWh and 566.5 kWh, respectively. As expected, the lowest EEG (276.1 kWh) is obtained in December because of low incident radiation (110.8 kWh). On average, the PVT panels generate 4% of the EEC in the cold months and 7% in the warm months.

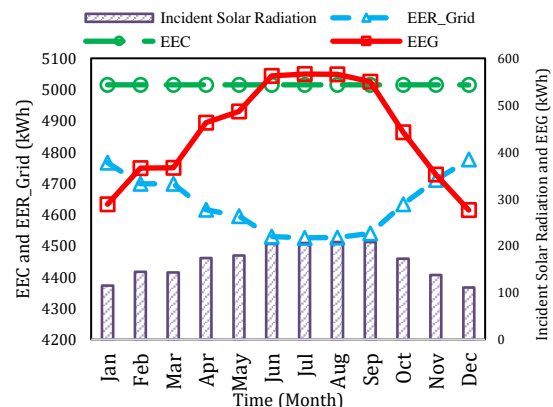


Figure 7. Monthly variation of incident solar radiation, EEG, EEC, and EER_Grid

Table 7 shows the annual electrical performance of the SCS. As can be seen, the annual EEC of the building is more than 60 MWh, of which about 54% is related to appliances (AEC) and the rest is related to lighting (LEC). The ratio of electrical energy received from the inverter (EER_Inv) to EEC is about 7.6%; however, the ratio of electrical energy received from the grid (EER_Grid) to EEC is 92.4%. It should be noted that the difference between the EEG and EER_Inv is because of the power loss in the system.

Table 7. Annual electrical performance of SCS

Parameter	Value (MWh)
Total electrical energy consumption (EEC)	60.18
Appliance electrical energy consumption (AEC)	32.60
Lighting electrical energy consumption (LEC)	27.58
Total electrical energy generation (EEG)	5.29
Electrical energy received from the grid (EER_Grid)	55.61
Electrical energy received from the inverter (EER_Inv)	4.57

Figure 8 shows the monthly variation of incident solar radiation, thermal energy generation (TEG), and consumption (TEC) including thermal energy consumption for providing DHW (DTEC) and SH (STEC). As observed, in warm months, almost all DHW load is provided by the SCS, because there is no need for SH. In the cold months, the STEC and thus, TEC have higher values, while TEG has lower values because of low incident radiation; so, the lowest TEG is obtained in December, which is 787 kWh. As can be seen, the ratio of STEC to TEG decreases from April and reaches zero from May to September, due to the lack of need for space heating. Nonetheless, it increases from October, so it is about 26 times larger in December compared to October. It is also found that the maximum ratio of TEC to TEG is 20.46 in January and the minimum one is 1.06 in August.

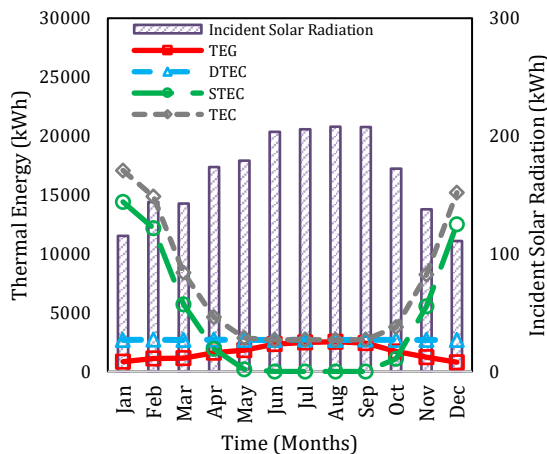


Figure 8. Monthly variation of incident solar radiation, TEG and, TEC

The annual thermal performance of the SCS is shown in Table 8. Based on the results, the annual TEC of the building is 89.57 MWh, of which about 60% is related to space heating (TEC_SH) and the rest is related to domestic hot water consumption (TEC_DHW). The ratio of TEG by the SCS to the TEC of the building is 22.5%.

Table 8. Annual thermal performance of SCS

Parameter	Value (MWh)
Total thermal energy consumption (TEC)	89.57
Thermal energy consumption for DHW (TEC_DHW)	32.57
Thermal energy consumption for SH (TEC_SH)	54.05
Total thermal energy generation (TEG)	20.13

The monthly variations of thermal, electrical, and total solar fractions of the SCS are shown in Figure 9. As the results show, in the warm months, due to the increase of incident solar radiation and the lack of need for SH, the thermal and total fractions have significantly grown. Due to the constant need for electricity, the monthly electrical fraction does not change much, but in the warmer months of the year, due to more radiation, a slight increase in the electrical fraction is observed.

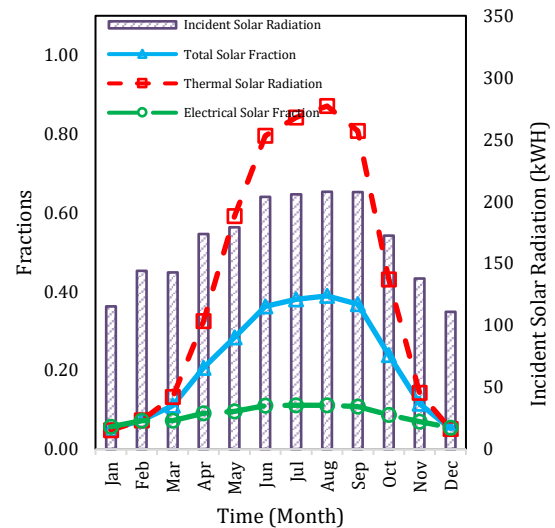


Figure 9. Monthly variation of different solar fractions

Conclusion

In this study, the performance of the SCS using PVT systems for supplying electricity, DHW, and SH demands of a case study building have been investigated and optimized using the Monte Carlo method. In the Monte Carlo method, by considering the risk conditions and calculating the probability of the

LCS, PBT, and IRR indicators, the optimum SCS system for the case study building is determined. The probability that the PBT is less than 5 years, the IRR is more than 20% and the LCS are more than the initial cost is 74.2%, 11.5%, and 97%, respectively. The analysis of the electrical performance of the optimum SCS indicates that a minimum of 5% and a maximum of 11% of the building's electrical load is provided by the system. The maximum electrical solar fraction is obtained from June to September. The annual electrical solar fraction of the SCS is 8.7%. In terms of thermal performance, it is found that the optimum SCS provided about 5%-87% of the building's thermal load. In the warm months (from April to October), about 66.6% of the building thermal demand is provided by the SCS; while, in the cold months (from November to March), on average 72% of the building thermal demand should be provided by fossil fuels. Finally, the maximum savings in electrical, thermal, and total energy consumption of the building using the optimum SCS are 11%, 87%, and 39%, respectively, which are related to the month of August. It is concluded that the optimization of the SCSs for providing the energy demands of the buildings leads to an efficient reduction of energy consumption.

It should be noted that a limitation of the research is the economic conditions of Iran and low price of the primary energies, which forced us to use the economic conditions and energy costs of the United States. It is recommended that the optimization of the SCS is performed for other climatic conditions and using other types of SCSs including different collector types and configurations of the storage tanks.

Nomenclature

d	Discount rate
F	Cash flow
N	Number
t	Time

Acronyms

AEC	Appliance Energy Consumption
DASC	Direct Absorption Solar Collector
DHW	Domestic Hot Water
DTEC	Domestic Thermal Energy Consumption
EEC	Electrical Energy Consumption

EEG	Electrical Energy Generation
EER	Electrical Energy Received
ETSC	Evacuated Tube Solar Collector
FPSC	Flat Plate Solar Collector
IRR	Internal Rate of Return
LCC	Life Cycle Cost
LCE	Life Cycle Energy
LCS	Life Cycle Savings
LEC	Lighting Energy Consumption
NPV	Net Positive Value
PBT	Payback Time
PVT	Photovoltaic-Thermal
PSO	Particle Swarm Optimization
SCS	Solar Combisystem
SH	Space Heating
TEC	Thermal Energy Consumption
STEC	Space Thermal Energy Consumption
TEG	Thermal Energy Generation
WWR	Windows-to-Wall Ratio

References

- [1] Karami, M., Raisee, M., and Delfani, S., 2014. Numerical investigation of nanofluid-based solar collectors. *IOP Conf. Ser.: Mater. Sci. Eng.*, 64 (1), 012044.
- [2] Amin, Z., Nematollahi, O., and Alemrajabi, A.A., 2021. Disinfection process with solar drying system. *Journal of Heat and Mass Transfer Research*, 8 (1), pp. 23-28.
- [3] Alamdari, P., Salihoglu, N.K., and Amin, Z., 2013. Solar energy potentials in Iran: A review. *Renewable and Sustainable Energy Reviews*, 21, pp. 778-788.
- [4] Hormozi Moghaddam, M. and Karami, M., 2022. Heat transfer and pressure drop through mono and hybrid nanofluid-based photovoltaic-thermal systems. *Energy Science & Engineering*, 10 (3), pp. 918-931.
- [5] Karami, M., Delfani, S., and Noroozi, A., 2020. Performance characteristics of a solar desiccant/M-cycle air-conditioning system

- for the buildings in hot and humid areas. *Asian Journal of Civil Engineering*, 21, pp. 189-199.
- [6] Leckner, M., Zmeureanu, R., 2011. Life cycle cost and energy analysis of a Net Zero Energy House with solar combisystem. *Applied Energy*, 88 (1), pp. 232-241.
- [7] Rasoul Asaee, S., Ismet Ugursal, V., Beausoleil-Morrison, I., Ben-Abdallah, N., 2014. Preliminary study for solar combisystem potential in Canadian houses. *Applied Energy*, 130, pp. 510-518.
- [8] Sustar, J. L., Burch, J., Krarti, M., 2015. Performance Modeling Comparison of a Solar Combisystem and Solar Water Heater. *J. Sol. Energy Eng.*, 137 (6), 061001.
- [9] Mehdaoui, F., Hazami, M., Messaouda, A., and Guizani, A.A., 2020. Performance analysis of two types of Solar Heating Systems used in buildings under typical North African climate (Tunisia). *Applied Thermal Engineering*, 165, 114203.
- [10] Hazami, M., Mehdaoui, F., Naili, N., Noro, M., Lazzarin, R., and Guizani, A. A., 2017. Energetic, exergetic and economic analysis of an innovative Solar CombiSystem (SCS) producing thermal and electric energies: Application in residential and tertiary households. *Energy Convers. Manag.*, 140, pp. 36-50.
- [11] Katsaprakakis, D. A. and Zidianakis, G., 2019. Optimized Dimensioning and Operation Automation for a Solar-Combi System for Indoor Space Heating: A Case Study for a School Building in Crete. *Energies*, 12 (1).
- [12] Karami, M. and Javanmardi, F., 2020. Performance assessment of a solar thermal combisystem in different climate zones. *Asian Journal of Civil Engineering*, 21, pp.751-762.
- [13] Karami, M. and Nasiri Gahraz, S.S., 2022. Improving thermal performance of a solar thermal/desalination combisystem using nanofluid-based direct absorption solar collector. *Sientia Iranica*, 29 (3), *Transactions on Mechanical Engineering (B)*, pp. 1288-1300.
- [14] Esmaeili, M., Karami, M. and Delfani, S., 2020. Performance enhancement of a direct absorption solar collector using copper oxide porous foam and nanofluid. *International Journal of Energy Research*, 44 (7), pp. 5527-5544.
- [15] Delfani, S., Karami, M., Akhavan-Behabadi, M.A., 2016. Experimental investigation on performance comparison of nanofluidbased direct absorption and flat plate solar collectors. *International Journal of Nano Dimension (IJND)*, 7 (1), pp. 85-96.
- [16] Karami, M. and Nasiri Gahraz, S.S., 2021. Transient simulation and life cycle cost analysis of a solar polygeneration system using photovoltaic-thermal collectors and hybrid desalination unit. *Journal of Heat and Mass Transfer Research*, 8 (2), pp. 243-256.
- [17] Kannan, A., Prakash, J., Roan, D., 2021. Design and performance of an off-grid solar combisystem using phase change materials. *International Journal of Heat and Mass Transfer*, 164, 120574.
- [18] Bornatico, R., Pfeiffer, M., Witzig, A. and Guzzella, L., 2012. Optimal sizing of a solar thermal building installation using particle swarm optimization. *Energy*, 41(1), pp. 31-37.
- [19] Hin, J.N.C. and Zmeureane, R., 2014. Optimization of a residential solar combisystem for minimum life cycle cost, energy use and exergy destroyed. *Solar Energy*, 100, pp. 102-113.
- [20] Rey, A. and Zmeureanu, R., 2016. Multi-objective optimization of a residential solar thermal combisystem. *Solar Energy*, 139, pp. 622-632.
- [21] Rey, A. and Zmeureanu, R., 2017. Micro-time variant multi-objective particle swarm optimization (micro-TVMOPSO) of a solar thermal combisystem. *Swarm and Evolutionary Computation*, 36, pp. 76-90.
- [22] Rey, A. and Zmeureanu, R., 2018. Multi-objective optimization framework for the selection of configuration and equipment sizing of solar thermal combisystems. *Energy*, 145, pp. 182-194.
- [23] Li, Y.H., Kao, W.C., 2018. Taguchi optimization of solar thermal and heat pump combisystems under five distinct climatic conditions. *Applied Thermal Engineering*, 133, pp. 283-297.
- [24] Thapa, B. and Wang, W., Williams, W., 2021. Life-cycle cost optimization of a solar combisystem for residential buildings in Nepal. *Journal of Asian Architecture and Building Engineering*, 21 (3), pp. 1137-1148.
- [25] Jalalizadeh, M., Fayaz, Rima, Delfani, S., Jafari Mosleh, H. and Karami, M., 2021. Dynamic simulation of a trigeneration system using an absorption cooling system and building integrated photovoltaic thermal solar collectors. *Journal of Building Engineering*, 43, 102482.
- [26] Goldsim. 2022. Monte Carlo Simulation. *Monte Carlo Simulation and Methods Introduction - GoldSim*.
- [27] Mun, J., 2006. Modeling risk: Applying Monte Carlo simulation, real options analysis, forecasting, and optimization techniques 347. John Wiley & Sons.
- [28] Fuller, S., 2010. Life-cycle cost analysis (LCCA). National Institute of Building Sciences, An Authoritative Source of

- Innovative Solutions for the Built Environment 1090.
- [29] Gu, Y., Zhang, X., Myhren, J. A., Han, M., Chen, X. and Yuan, Y., 2018. Techno-economic analysis of a solar photovoltaic/thermal (PV/T) concentrator for building application in Sweden using Monte Carlo method. *Energy Convers. Manag.* 165, pp. 8-24.
- [30] Kalogirou, S., 2014. *Solar Energy Engineering: Processes and Systems*, Academic Press, second edition.